Channel measurement and time dispersion analysis for outdoor mobile ultrawideband environment

Solomon NUNOO[1,2,*], **Uche A.K. CHUDE-OKONKWO**[1], **Razali NGAH**[1],
Chollette CHUDE-OLISAH[3], **Yasser K. ZAHEDI**[1]
[1]Wireless Communication Centre, Universiti Teknologi Malaysia, Johor, Malaysia
[2]Department of Electrical and Electronic Engineering, University of Mines and Technology, Tarkwa, Ghana
[3]Faculty of Computing, Universiti Teknologi Malaysia, Johor, Malaysia

Abstract: Ultrawideband (UWB) technology offers short-range high-data transmission rates. Most researchers in recent times have focused on indoor UWB channel measurements and in instances where outdoor cases were reported, they focused on static scenarios. This paper reports on mobile outdoor channel measurements typical of roadway and recreation park Infostation scenarios. It also chronicles the delay spread as well as channel stationarity analysis of the measurement data. We carried out measurements in the 3.1–5.3 GHz frequency range in various line-of-sight scenarios. The results of this research show that the delay spread values generally decrease with increasing mobile speed. Additionally, the degree of variation in the channel statistics show that systems designed with the obtained reference parameter values will perform well on average, but with low resource utilization.

Key words: Ultrawideband, channel measurement, Infostation, time dispersion, channel stationarity.

1. Introduction

Several studies have arisen in recent times in the area of ultrawideband (UWB) communication as a result of its established potential capabilities in high-speed and short-range wireless applications. One such application is the Infostation network [1–4]. The Infostation network can be located in diverse areas and in different user-defined scenarios such as sit-through, walk-through, and drive-through scenarios. The drive-through scenario depicts a situation where users pass through the coverage area in seconds at high speed, as in a roadway and railway; the walk-through scenario characterizes slow-moving users, such as in airports, on sidewalks, or at malls; and finally the sit-through scenario refers to stationary users, such as those in a classroom [4]. Scenarios that can benefit from Infostation service are locations where users can download/upload high-quality videos/images/data with large data size in a matter of seconds while sitting/walking around a recreation park as illustrated in Figure 1. Traditionally, the Infostation definition considers sequential user access with discontinuous coverage areas [5]. However, with the inherent high data rate of UWB communication and the performance of the various multiple access techniques proposed by Foerster [6] and Win and Scholtz [7], multiuser Infostation applications are feasible. The advent of technologies such as the UWB radio-over-fiber [8] will also enable such application scenarios.

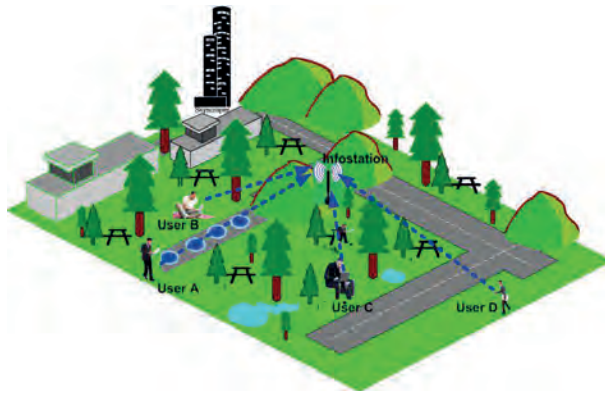---

*Correspondence: snunoo@ieee.org

Figure 1. Illustration of Infostation environment in a park.

Like in any other communication system, one of the classical foci of the UWB system design is the impact of the wireless channel on the received signal. Prior to system deployment, system designers require adequate knowledge of the propagation environment. The required knowledge of channel characteristics can be obtained by measurement and modeling. We can categorize typical Infostation propagation environments as either indoor or outdoor. A large literature base on UWB indoor measurements is available, some of which can be found in [9–12]. However, to the best of our knowledge, the number of outdoor measurement campaigns presented in the literature is limited. Some of the existing works on outdoor measurement campaigns can be found in [13–17]. Apart from the outdoor measurement in a gas station and drive-through restaurant [17], and a roadway and parking lot [12], no other literature on UWB measurement in an Infostation scenario is available. This paper aims to provide measurements to fill in the gap.

Usually, the data obtained from the measurement are analyzed and some specific channel parameters are obtained. These channel parameters are further used to define the parameters required for the design of the communication system. Some of the channel parameters of interest include the mean delay spread τ_M, root-mean-square (RMS) delay spread τ_{RMS}, coherence time T_C, coherence bandwidth B_C, and maximum Doppler spread $v_{\max}$ [18]. Basically, τ_{RMS}, τ_M, and B_C account for the time dispersion of the channel, while $v_{\max}$ and T_C account for the frequency dispersive characteristics of the channel. In system design, these channel parameters are used to define things like the step-size update interval for adaptive channel estimation algorithms, the choice of pilot spacing, frame length, data rate, and, in multicarrier systems, the subcarrier spacing.

In a real sense, channel parameter values depend on the transmitter and receiver separation distance, the position of scatterers, the speed of the communication terminals/scatterers, and the transmit power. Hence, obtained values for these channel parameters may vary greatly depending on environments and locations. In the case of the recreation park scenario, channel parameter values may vary from one sitting location to another, and from one position to another as a user walks around the park. The worst-case scenario approach is always used for conventional system design when choosing effective system parameter values from the channel measurement results [19]. This pessimistic approach may simplify the design of transceivers, but merely assures average performance, since resources are often underutilized. However, if we can estimate the range of the values over which the channel parameters do not fluctuate considerably, we may be able to incorporate such information into the system design. For instance, we can enhance the performance of a transceiver subsystem by using adaptive algorithms via available channel information.

We can obtain information on a channel's variability if we can quantify the degree of the channel's stationarity from the measurement data. In all existing literature, the analysis of time dispersion characteristics of the UWB channel does not include stationarity attributes of measured data. This paper differs significantly from our earlier work on the characterization and parameterization of dynamic wireless channels using evolutionary channel parameters [19] in that it focuses on the time dispersion analysis of UWB channel measurements in two separate outdoor mobile scenarios. Hence, the following are our major contributions in this paper:

- We carried out a set of time domain measurements of an UWB channel typical of a multiuser Infostation in an outdoor roadway and recreation park.

- We also present time dispersion analysis of the measured data with particular emphasis on the concept of channel statistical stationarity.

The following itemizes the organization of the rest of this paper. In Section 2 we discuss time dispersion characteristics of the Infostation channel in various measurement environments in terms of delay spread and coherence bandwidth, as well as channel stationarity analysis. Section 2 concludes by enumerating the significance of the stationarity concept to system design. We discuss measurement setup in Section 3. Section 4 presents a description of the measurement environments as well as the procedure for the measurement. Section 5 highlights an application example and simulation results. Finally, we conclude and state future works in Section 6.

2. Time dispersion analysis

We consider the analysis of time dispersion characteristics of the Infostation channel in various environments measured. Time dispersion is a characteristic of a multipath channel that extends the signal in time so that the duration of the received signal is greater than the transmitted signal. These parameters, τ_{RMS}, τ_M, and B_C, usually capture this effect. In addition, to capture the degree of channel variation, stationarity parameters suffice.

2.1. Delay spread and coherence bandwidth analysis

It is possible to determine τ_{RMS} and τ_M using the power delay profile (PDP) of the channel. τ_{RMS} is the square root of the second central moment, while τ_M is the first moment of the PDP. If we represent the PDP at the kth delay as $P(\tau_k)$, then τ_{RMS} is expressed with respect to the second-order moment as [18]:

$$\tau_{RMS} = \sqrt{\overline{\tau^2} - \left(\tau_M\right)^2}, \tag{1}$$

where

$$\tau_M = \frac{\sum\limits_{k} P^2\left(\tau_k\right)\tau_k}{\sum\limits_{k} P^2\left(\tau_k\right)} \tag{2}$$

and

$$\overline{\tau^2} = \frac{\sum\limits_{k} P^2\left(\tau_k\right)\tau_k^2}{\sum\limits_{k} P^2\left(\tau_k\right)}. \tag{3}$$

The corresponding coherence bandwidth, defined as the frequency range over which the channel is considered flat, is given at 50% correlation by:

$$B_C = \frac{1}{5\tau_{RMS}}.$$

(4)

The values of τ_{RMS} are used to set the appropriate value for the symbol duration for a given system and, invariably, the data rate. In multicarrier systems, both τ_{RMS} and B_C are used to set the value of the guard interval and the subcarrier spacing, respectively.

2.2. Channel stationarity analysis

While the characterization of time dispersion of wireless channels using τ_{RMS} and B_C is common, both parameters do not offer a comprehensive approach when characterizing all classes of time-varying processes. Undeniably, the concept of coherency describes the nonselectivity of WSSUS channels. In this sense, the stationarity attribute of the WSSUS channel is infinite. Consequently, over certain bounded values, the channel is coherent in both frequency and time. Moreover, we assume that the channel remains stationary (i.e. statistically invariant) in frequency and time to an infinite extent. This is not always the case in most measurement (practical) results; for example, the degree of channel stationarity is finite. Hence, in practice, one often has to resort to the assumption that channel statistics can remain almost constant with a stationarity dimension in time and bandwidth.

A number of perspectives have been used in the literature to assess the stationarity dimension of the time-varying channel. Some are based on the variation in first-order statistics [20], while others are based on second-order statistics of the channel [20–22]. In [20] the stationarity region, termed the local region of stationarity (LRS), was defined based on the change of the PDP $P_{\mathrm{H}}(t, \tau)$ with respect to locations. The LRS is the geographical region where, starting from its maximum value, a correlation coefficient $C(t_i, \Delta t)$ does not go below a certain threshold. The temporal correlation coefficient at time instants t_i, $i = 1, 2, 3, \ldots, I$ is expressed as:

$$C(t_i, \Delta t) = \frac{\int \overline{P_{\mathbf{H}}(t_i, \tau)} \cdot \overline{P_{\mathbf{H}}(t_i + \Delta t, \tau)} d\tau}{\max\left\{\int \overline{P_{\mathbf{H}}(t_i, \tau)}^2 d\tau, \int \overline{P_{\mathbf{H}}(t_i + \Delta t, \tau)}^2 d\tau\right\}}.$$

(5)

Within a classical theoretical framework, Matz [21] introduced the stationarity bandwidth and time, which are based on the concept of non-WSSUS. The stationarity time and stationarity bandwidth are defined as Doppler spread weighted integrals and the inverse of some normalized maximum delay, respectively. The stationarity bandwidth F_S and time T_S, at some delay τ and Doppler shift υ, are defined within a level-ε stationarity region $\Re_S^\varepsilon(t_0, f_0)$ at some point (t_0, f_0) on a time (t)-frequency (f) plane such that [21]:

$$\Re_S^\varepsilon(t_0, f_0) = \left[t_0 - \varepsilon\frac{T_S}{2}, t_0 + \varepsilon\frac{T_S}{2}\right] \times \left[f_0 - \varepsilon\frac{F_S}{2}, f_0 + \varepsilon\frac{F_S}{2}\right],$$

(6)

where

$$T_S = \left(\frac{1}{\|A_H\|_1} \iiiint w_1(\Delta t, \Delta f; \Delta\tau, \Delta\upsilon) \times |A_H(\Delta t, \Delta f; \Delta\tau, \Delta\upsilon)| \, d\Delta t \, d\Delta f \, d\Delta\tau \, d\Delta\upsilon\right)^{-1},$$

(7)

$$F_S = \left(\frac{1}{\|A_H\|_1} \iiiint w_2(\Delta t, \Delta f; \Delta\tau, \Delta\upsilon) \times |A_H(\Delta t, \Delta f; \Delta\tau, \Delta\upsilon)| \, d\Delta t \, d\Delta f \, d\Delta\tau \, d\Delta\upsilon\right)^{-1}.$$

(8)

A_{H} is the channel correlation function. If we consider the maximum extension in delay and Doppler lag for which $A_{\mathrm{H}}\left(\Delta t, \Delta f ; \Delta \tau, \Delta v\right) \neq 0$, then the stationarity bandwidth and stationarity time can simply be given as:

$$\bar{F}_S = \frac{1}{\Delta \tau_{\max}}, \quad F_S \geq \bar{F}_S, \tag{9}$$

$$\bar{T}_S = \frac{1}{\Delta v_{\max}}, \quad T_S \geq \bar{T}_S, \tag{10}$$

where $\bar{T}_S$ is interpreted as the time lag within which stationarity is assumed for a given stationarity length and mobile speed. Given that the correlation of different delay components is only a result of scattering from the same physical object, $\bar{F}_S$ can be interpreted as the ratio of the speed of the wave to the dimension of the object.

The stationarity parameters described above are generally computed from a single recorded channel, which is the average of a set of channel realizations taken over a specific duration. The average channel realization is then analyzed using a multitaper-based estimator [21]. This estimator slides a separable window function that comprises two prolate spheroidal functions in time and frequency over the recorded channel. However, the choice of the two window functions in time and frequency may present conflicting requirements with respect to the Heisenberg uncertainty principle.

In an alternative approach, and inspired by Matz [21], the concept of local-sense stationary uncorrelated scattering (LSSUS) was introduced by Chude-Okonkwo et al. [22]. The LSSUS concept was used to define the stationarity bandwidth and time using the definition of minimal RMS delay spread deviation $\Delta \tau_{RMS}$ and minimal scale spread deviation $\Delta s_{\max}$ for wideband channels (and consequently minimal Doppler spread deviation for narrowband, if required), respectively. The values $\Delta \tau_{RMS}$ and $\Delta s_{\max}$ were alternatively defined as deviations in delay (τ) and scale (s) (in relation to Doppler spread) of a given LSSUS channel realization from the reference WSSUS values. The expression for the LSSUS scattering function, which is an evolutionary spectrum, is given by Chude-Okonkwo et al. [22]:

$$\mathbf{P}_{LSSUS}\left(\tau, s ; \Delta \vec{r}\right) = \left\langle R_y, X^{(\tau, s)}_{\Delta(\tau+\Delta\tau)+\Delta\tau, \Delta(s+\Delta s)+\Delta s}\right\rangle_{\Delta(t+\Delta t)+\Delta t}, \tag{11}$$

where $X^{(\tau, s)} = a(t)x\left(\frac{t-\tau}{s}\right)$ is a copy of the delay (by τ)-scaled (by s)-attenuated (by a) version of the probe signal $x(t)$ and $y(t)$ is the received signal. The values of $\Delta\tau$, Δs, and Δt are controlled by the position vector $\Delta \vec{r}$ where $\Delta \vec{r} = \Delta t.v$. The value of $\Delta \vec{r}$ is synonymous to the repetition distance in real-time measurement and hence is regarded as the maximal stationarity distance.

For negligible change in the position of the receiver/transmitter, the LSSUS and WSSUS functions become equivalent, such that:

$$\mathbf{P}_{WSSUS}\left(\tau, s\right) = \mathbf{P}_{LSSUS}\left(\tau, s ; \Delta \vec{r} \rightarrow 0\right)|_{\Delta t, \Delta \tau, \Delta s \rightarrow 0}. \tag{12}$$

Hence, to quantify the deviation of LSSUS from WSSUS, the minimal delay profile deviation (MDPD) Ξ_τ^2 and the minimal scale profile deviation (MSPD) Ξ_S^2 are defined and expressed as [22]:

$$\Xi_\tau^2 = \min_{\check{\mathbf{P}}_{WSSUS}} \iint \left(\mathbf{P}_{LSSUS}\left(\tau, s\right) - \mathbf{P}_{WSSUS}\left(\tau, s\right)\right)^2 \frac{ds}{s^2}, \tag{13}$$

$$\Xi_S^2 = \min_{\check{\mathbf{P}}_{WSSUS}} \iint \left(\mathbf{P}_{LSSUS}\left(\tau, s\right) - \mathbf{P}_{WSSUS}\left(\tau, s\right) \right)^2 d\tau. \tag{14}$$

Consequently, the extension in delay and scale are termed the minimal RMS delay spread deviation $\Delta\tau_{RMS}$ and minimal scale spread deviation $\Delta s_{\max}$ and are given by:

$$\Delta\tau_{RMS} = \left(\frac{\int \left(\Xi_{\tau,LSSUS}^2 \tau^2 - \Xi_\tau^2 \tau^2 \right) d\tau}{\int \Xi_{\tau,LSSUS}^2 d\tau} - \left(\frac{\int \left(\Xi_{\tau,LSSUS}\tau - \Xi_\tau\tau \right) d\tau}{\int \Xi_{\tau,LSSUS}^2 d\tau} \right)^2 \right)^{1/2} - \\ \cdot \left(\frac{\int \left(\Xi_{\tau,WSSUS}^2 \tau^2 - \Xi_\tau^2 \tau^2 \right) d\tau}{\int \Xi_{\tau,WSSUS}^2 d\tau} - \left(\frac{\int \left(\Xi_{\tau,WSSUS}\tau - \Xi_\tau\tau \right) d\tau}{\int \Xi_{\tau,WSSUS}^2 d\tau} \right)^2 \right)^{1/2} , \tag{15}$$

$$\Delta s_{\max} = s_{\max,LSSUS} - s_{\max,WSSUS}, \tag{16}$$

where

$$\Xi_{\tau,WSSUS}^2 = \min_{\check{\mathbf{P}}_{WSSUS}} \iint \left[\mathbf{P}_{LSSUS}\left(\tau, s\right) - \mathbf{P}_{WSSUS}\left(\tau, s\right) \right]^2 \frac{ds}{s^2} \bigg|_{\mathbf{P}_{LSSUS}(\tau,s)=0} \tag{17}$$

and

$$\Xi_{\tau,LSSUS}^2 = \iint \left[\mathbf{P}_{LSSUS}\left(\tau, s\right) - \mathbf{P}_{WSSUS}\left(\tau, s\right) \right]^2 \frac{ds}{s^2} \bigg|_{WSSUS(\tau,s)=0} . \tag{18}$$

Hence, the stationarity bandwidth $\bar{F}_S = \frac{1}{|\Delta\tau_{RMS}|}$ and stationarity time $\bar{T}_S = \frac{1}{|\Delta s_{\max}|f_R}$, where f_R is the reference frequency component of the probe signal. In narrowband systems f_R is the center frequency, and in wideband systems like the UWB, f_R is the maximum frequency component. In this case, $\bar{F}_S$ and $\bar{T}_S$ are simply computed as the inverse of the difference in delay and Doppler shifts, respectively, between a reference channel realization (snapshot) and the rest of the snapshots. This is physically related to comparing a reference value of second-order statistics with other possible values for a given channel.

2.3. Significance of stationarity concepts to system design

Having defined the concepts of stationarity parameters according to the perspectives of different authors, the major concern of a system designer is how the stationarity parameters can be of benefit to the system design. Four major implications of the stationarity definition of Matz [21] and Chude-Okonkwo et al. [22] are:

- The dimension $\bar{T}_S \times \bar{F}_S$ can be used to ascertain the ergodicity of a given channel in terms of the number of independent fading realizations.

- The dimension $\bar{T}_S \times \bar{F}_S$ can be used to ascertain whether a channel is doubly underspread (DU) or not.

- Within the time intervals of duration $\bar{T}_S$ and frequency bands of width $\bar{F}_S$, if the channel is DU, then it can locally be approximated by (properly chosen) WSSUS channels.

- DU channel validation simplifies the design since it allows one to separate the randomness and the TF variations of the channel via a 2-D Karhunen–Loeve expansion involving a simple TF localization filter, TF shifts, and uncorrelated random weights.

In the context of Gehring et al. [20], the definition of the stationarity dimension is very handy when we consider the design of modules that are very sensitive to sudden changes in channel coefficients. For instance, systems such as the UWB that employ Rake receivers are extremely sensitive to sudden change in channel response. Hence, development of Rake models that are robust against this sudden channel variation is necessary. Information necessary for the efficient design of such models can be obtained from LRS analysis.

The definition of stationarity in [22] informs about how much the second-order statistics of a reference channel deviate from another channel realization. Hence, the values of the stationarity parameters depend on the reference channel realization chosen. In the next section, the ensuing time dispersion analysis will consider this version of the definition of channel stationarity.

3. Measurement setup

To obtain channel response, we carried out the measurements in the time domain. The sounding system used consisted of a pair of PulsON 410 (P410) transceivers. This system maintains the phase information of each pulse using coherent transmissions. This makes it possible to capture the received waveform devoid of a wired link between the receiving and transmitting sides. The antenna used for each P410 transceiver system was a vertically polarized omnidirectional wideband (3.1–10.6 GHz) dipole antenna. For all the measurement scenarios under consideration, the location of the transmitting antenna, which served as the access point (AP), was 2.5 m above the ground. The transceiver system transmitted over a frequency range of 3.1–5.3 GHz, which resulted in a pulse bandwidth of 2.2 GHz. The step size used was 32 and this allowed the system to make one measurement every 61 ps. The duration of a snapshot was approximately 99.609375 ns, which resulted in about 1632 bins.

4. Measurement environment and procedure

All the measurement environments were along a roadway and at a recreation park located inside the Johor campus of Universiti Teknologi Malaysia as shown in Figure 2. For simplicity, we named the roadway and the recreation park environments as Environment A and Environment B, respectively. We conducted the measurements very early in the morning to minimize the influence of scatterers' mobility.

(a) Environment A   (b) Environment B

Figure 2. Google maps of measurement environments: (a) Environment A, (b) Environment B.

4.1. Environment A

This environment is a roadway located within the vicinity of Block P16, which houses a number of lecture halls within the university. Figure 3 shows Block P16 with the roadway in front of it; the dark arrow points to the location of the AP. As shown, one side of the roadway has a building complex and the other side has vegetation on a slope. Figure 4 also illustrates a sketch of the setup for the measurement. Two channel scenarios are discussed for Environment A, namely CH1 and CH2.

Figure 3. Environment A: roadway measurement environment.

We placed the transmitter at the edge of the roadway and took the measurements under two separate mobile scenarios: at a speed of 0.8 m/s in the first scenario and 1.2 m/s in the second. The height of the receiver was 1 m from the ground throughout this measurement and we moved it along a predefined straight path on the roadway. Let us fit in a virtual straight line that cuts through the transmitter location. This virtual straight line is equidistance to the measurement routes for CH1 and CH2, with separation distances of 3.5 m and 10 m, respectively. We moved a distance of 80 m along the CH1 and CH2 routes. The captured channel impulse response (CIR) averaged 235 and 135 samples for 0.8 m/s and 1.2 m/s, respectively.

The choice of continuous movement for the measurement was made to imitate a typical situation whereby a person moves within an Infostation network. In addition, we chose the 80-m measurement route to indicate a challenging coverage radius of 40 m.

4.2. Environment B

This environment is a section of the recreation park and is represented by the area indicated by the white circle in the Google map shown in Figure 2. It depicts a typical scenario in the park where people sit at different locations and download/upload information from/to the same AP in an Infostation network. We considered 5 different designated sitting areas, each enclosed in a circle with a radius of 1 m. We designated these five areas as G_1, G_2, G_3, G_4, and G_5. The centers of the circular areas that enclose G_1, G_2, G_3, G_4, and G_5 are about 12 m, 29 m, 25 m, 10 m, and 29 m, respectively, from the transmitter (akin to the AP) as shown in Figures 5–9. Note that the location of the transmitter is close to the red signboard in the photos. In all cases, the receiver is located 1 m above the ground, which depicts a typical scenario where the user is sitting on a bench. We use the dark arrows, shown in Figures 5–9, to point out the individual sitting positions for each scenario. We situated area G_2 on a platform somewhere close to the middle of the lake in the park, while the rest of the areas are situated off the lakeshore. We recorded an average of 50 CIRs at random positions at each location.
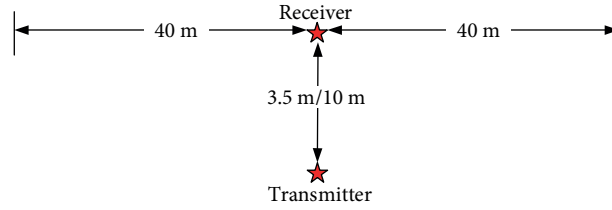
Figure 4. Environment A: sketch of the setup for collecting propagating data.

Table 1. Delay spread measurement results for Environment A.

Channel	Speed (m/s)	τ_{RMS} (ns)		τ_M (ns)	
		Range	Average	Range	Average
CH1	0.8	0.6–35.1	9.902	8.4–96.6	51.46
	1.2	0.6–32.7	9.181	3.7–95.6	49.95
CH2	0.8	1.2–23.0	9.953	16.1–93.9	63.69
	1.2	2.1–23.8	9.905	21.8–89.8	63.73

Table 2. Correlation coefficient results for Environment A.

Channel	Speed (m/s)	Correlation coefficient			
		τ_{RMS}	$\bar{F}_{S,ref.A}$	$U_{Ref.M}$	$U_{Ref.A}$
CH1	0.8	−0.7258	−0.5431	0.4223	0.4393
	1.2	−0.6946	−0.4095	0.3851	0.3957
CH2	0.8	−0.6551	−0.1127	0.4174	0.4225
	1.2	−0.6278	−0.2241	0.4464	0.4609

To quantify the extent to which the channel statistics vary, following Chen et al. [23], we define the percentage of the deviation U of the channel statistics with respect to a reference location X as:

$$U = \left(\frac{5B_{C,X}}{B_{S,ref.X}} \right) \times 100, \tag{19}$$

where the factor 5 accounts for the 50% correlation requirement for the computation of $B_{C,X}$. The $B_{S,ref.X}$ term is the stationarity bandwidth computed without considering the magnitude of $\Delta\tau_{RMS}$ such that $B_S = 1/\Delta\tau_{RMS}$.

Let Channel A and Channel M represent the reference channels at the start of the measurement run and the channel at which the maximum τ_{RMS} value is recorded, respectively. The values of the stationarity bandwidth $\bar{F}_{S,ref.A}$ and the values of U associated with $B_{S,ref.A}$ and $B_{S,ref.M}$ are shown in Figures 12 and 13, respectively. Table 2 shows the correlation coefficient results between $\bar{F}_{S,ref.A}$, $U_{Ref.M}$, and $U_{Ref.A}$ and distance for CH1 and CH2.

5. Results of time dispersion analysis for measurement data

Typical CIRs measured during the experiment are shown in Figure 10. The CIRs were obtained by deconvolving the template waveform from the measured signal using the CLEAN algorithm at a 25-dB threshold.

The range and average values of the measured τ_{RMS} and τ_M for Environment A are given in Table 1. The plot of the τ_{RMS} values with respect to distance is shown in Figure 11. High τ_{RMS} values observed at the 0–25 m mark in the four channel scenarios are due to the influence of a set of structures in the vicinity. Notable

Figure 5. Environment B: measurement environment for G_1.

Figure 6. Environment B: measurement environment for G_2.

Figure 7. Environment B: measurement environment for G_3.

Figure 8. Environment B: measurement environment for G_4.

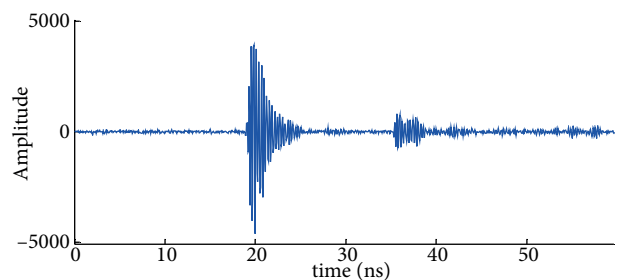**Figure 9.** Environment B: measurement environment for G_5.

Figure 10. Typical CIR captured in the measurement.

among them is a road sign erected at a height of 1.5 m above ground level. The correlation coefficient results between τ_{RMS} and distance for CH1 and CH2 are shown in Table 2. The results for CH1 indicate a strong downhill linear relationship when the speed of movement is 0.8 m/s and a moderate downhill relationship when the speed of movement is 1.2 m/s. In the case of CH2, the results indicate a moderate downhill relationship in both cases. Thus, we deduce that the correlation between τ_{RMS} and distance decreases with increasing mobile speed.
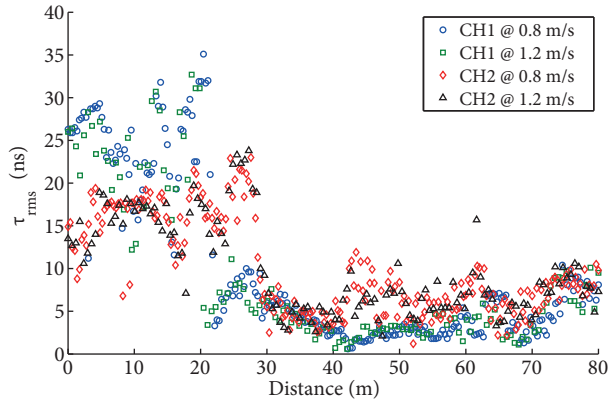
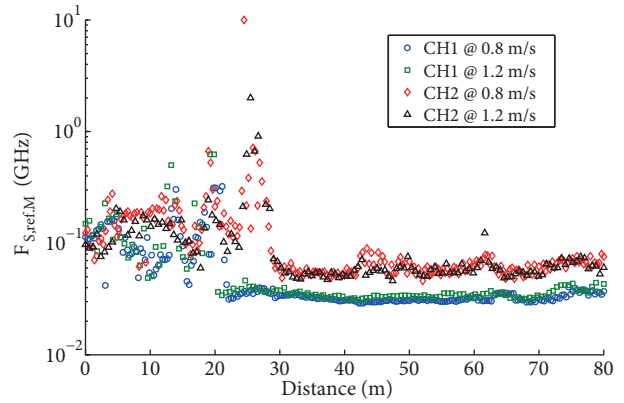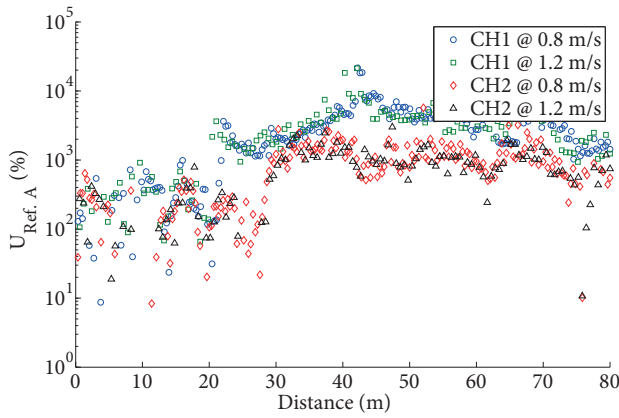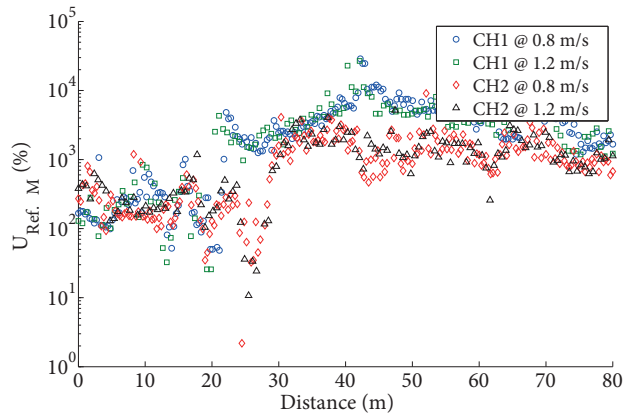**Figure 11.** RMS delay spread vs. distance for Environment A.

Figure 12. Stationarity bandwidth vs. distance in Environment A.

(a) $U_{Ref.A}$vs. distance

(b) $U_{Ref.M}$vs. distance

Figure 13. Percentage of deviation vs. distance in Environment A: (a) $U_{Ref.A}$ vs. distance, (b) $U_{Ref.M}$ vs. distance.

With regard to Environment B, the range and mean values of τ_{RMS} and τ_M measured at locations G_1, G_2, G_3, G_4, and G_5 in the park are given in Table 3. The corresponding values of the B_C, $\bar{F}_{S,ref.G_1}$, and U with respect to the channel at G_1 are given in Table 4.

Table 3. Delay spread measurement results for Environment B.

Location	Distance (m)	Range τ_{RMS}	Average τ_{RMS} (ns)	τ_M (ns)
G_1	12	0.6–4.6	3.13	0.291
G_2	29	0.9–19.9	8.68	1.273
G_3	25	5.8–12.9	9.32	1.987
G_4	10	2.1–7.2	3.91	0.413
G_5	29	0.8–28.5	14.37	1.192

Table 4. Coherence bandwidth and stationarity parameters for Environment B.

Position	B_C (MHz)	$\bar{F}_{S,ref.G_1}$ (MHz)	U (%)
G_1	63.94	∞	0
G_2	23.06	180.3	-63.94
G_3	21.47	161.6	-66.43
G_4	51.12	1282.9	-19.95
G_5	13.92	89.0	-78.23

The degree of variation in channel statistics is clearly observable in U. In Figure 13 it can be seen that most of the values of time dispersion parameters differ from the values at channel A ($U = 0\%$) in most cases. We also observe large deviations for Environment B in most cases as summarized in Table 3. A negative value of U indicates overutilization of bandwidth resources whereas a positive value indicates underutilization of bandwidth resources.

For instance, let us consider the spectral efficiency η of a multicarrier system expressed as [24]:

$$\eta = \frac{1}{1 + \Delta f \left(T_g + T_{cp}\right)}, \tag{20}$$

where T_{cp} is the duration of cyclic prefix, Δf is the subcarrier spacing, and T_g is the guard interval. The value of T_g is selected to be such that it always allows a respectable time interval for the receiver and transmitter to change to the next carrier frequency.

The value of T_{cp} should also be selected such that it ensures that intersymbol interference (ISI) is mitigated [25,26]. The standard value of T_{cp} according to IEEE 802.15.3a is 60.61 ns [25,26]. In essence, the rule of thumb for choosing T_{cp} is that it must be equal to or greater than the maximum delay spread, or $T_{cp} > k\tau_{rms}$, $k = 2, 3, ...$ This is to ensure the elimination of ISI at any possible high value of delay spread. For the conventional value of $\Delta f = 4.125$ MHz and $T_g = 9.47$ ns, using Eq. (20), the average value of η for the IEEE 802.15.3a standard is approximately 0.776. To enhance performance, the value of U can be incorporated into Eq. (20) and thus:

$$\eta = \frac{1}{1 + \Delta f \left(T_g + aT_{cp,ref}\right)}; \quad a = 1 + U/100, \tag{21}$$

where $T_{cp,ref}$ is the value of $T_{cp} > k\tau_{rms}$ at the reference channel.

If the transceiver for the park environment is designed with adaptive parameters specified by channel G_1, then for $k = 10$ the spectral efficiencies at G_1, G_2, G_3, G_4, and G_5 are 0.8560, 0.9211, 0.9239, 0.8753, and 0.9371, respectively, with an average value of 0.9027. Hence, by incorporating the stationarity information via stationarity parameters, system performance can be improved in an adaptive fashion.

6. Conclusion

We presented UWB channel measurement results in an outdoor recreation park. Specifically, the measurement procedure mimics typical Infostation scenarios envisaged for information access in a roadway and recreation park. We carried out an analysis of the measured channel with respect to the delay spread and stationarity parameters. Finally, we presented an illustration of the benefits of employing stationarity information in system design for performance improvement. As future work, we will develop algorithms that can estimate the mobile UWB channel adaptively.

Acknowledgment

References

[1] Frenkiel RH, Badrinath BR, Borres J, Yates RD, Borras J. The infostations challenge: balancing cost and ubiquity in delivering wireless data. IEEE Pers Commun 2000; 7: 66-71.

[2] Galluccio L, Leonardi A, Morabito G, Palazzo S. Timely and energy-efficient communications in rural infostation systems. IEEE Wirel Commun 2008; 15: 48-53.

[3] Rajappan G, Acharya J, Liu H, Mandayam N, Seskar I, Yates R. Mobile infostation network technology. In: Proceedings of SPIE on Wireless Sensing and Processing; 17–18 April 2006; Orlando, FL, USA.

[4] Cavalcanti D, Sadok D, Kelner J. Mobile infostations: a paradigm for wireless data communications. In: Wireless and Optical Communications; 17–19 June 2002; Banff, Canada.

[5] Iacono AL, Rose C. Infostations: new perspectives on wireless data networks. In: Tekinay S, editor. Next Generation Wireless Networks. Boston, MA, USA: Kluwer Academic Publishers, 2002. pp. 3-63.

[6] Foerster JR. The performance of a direct-sequence spread ultrawideband system in the presence of multipath, narrowband interference, and multiuser interference. In: 2002 IEEE Conference on Ultra Wideband Systems and Technologies; 21–23 May 2002; Baltimore, MD, USA. pp. 87-91.

[7] Win MZ, Scholtz RA. Ultra-wide bandwidth time-hopping spread-spectrum impulse radio for wireless multiple-access communications. IEEE T Commun 2000; 48: 679-689.

[8] Wah MY, Yee C, Yee ML. Wireless ultra wideband and communications using radio over fiber. In: IEEE Conference on Ultra Wideband Systems and Technologies; 16–19 November 2003; Reston, VA, USA. pp. 265-269.

[9] Noori N, Karimzadeh-Baee R, Abolghasemi A. An empirical ultra wideband channel model for indoor laboratory environments. Radioengineering 2009; 18: 68-74.

[10] Donlan BM, McKinstry DR, Buehre RM. The UWB indoor channel: large and small scale modeling. IEEE T Wirel Commun 2006; 5: 2863-2873.

[11] Cramer RJM, Scholtz RA, Win MZ. Evaluation of an ultra-wide-band propagation channel. IEEE T Antenn Propag 2002; 50: 561-570.

[12] Lee JY. UWB channel modeling in roadway and indoor parking environments. IEEE T Veh Technol; 59: 3171-3180.

[13] Di Francesco A, Di Renzo M, Feliziani M, Graziosi F, Manzi G, Santucci F, Minutolo R, Presaghi R. Sounding and modelling of the ultra wide-band channel in outdoor scenarios. In: 2nd International Workshop on Networking with Ultra Wide Band and Workshop on Ultra Wide Band for Sensor Networks; 4–6 July 2005; Rome, Italy. pp. 20-24.

[14] Win MZ, Ramirez-Mireles F, Scholtz RA, Barnes MA. Ultra-wide bandwidth (UWB) signal propagation for outdoor wireless communications. In: 1997 IEEE 47th Vehicular Technology Conference; 4–7 May 1997; Phoenix, AZ, USA. pp. 251-255.

[15] Kim CW, Sun X, Chiam LC, Kannan B, Chin FPS, Garg HK. Characterization of ultra-wideband channels for outdoor office environment. In: IEEE Wireless Communications and Networking Conference; 13–17 March 2005; New Orleans, LA, USA. pp. 950-955.

[16] Souza CF, Bello JCRD. UWB signals transmission in outdoor environments for emergency communications. In: 2008 11th IEEE International Conference on Computational Science and Engineering – Workshops; 16–18 July 2008; Sao Paulo, Brazil. pp. 343-348.

[17] Santos T, Karedal J, Almers P, Tufvesson F, Molisch AF. Modeling the ultra-wideband outdoor channel: measurements and parameter extraction method. IEEE T Wirel Commun 2010; 9: 282-290.

[18] Molisch AF. Wireless Communications. 2nd ed. West Sussex, UK: John Wiley & Sons, 2011.

[19] Chude-Okonkwo UAK, Chude-Olisah CC, Nunoo S, Nga R. Characterization and parameterization of dynamic wireless channels over long duration using evolutionary channel parameters. Int J Commun Syst 2015; 29: 893-915.

[20] Gehring A, Steinbauer M, Gaspard I, Grigat M. Emperical channel stationarity in urban environments. In: 4th European Personal Mobile Communications Conference; 20–21 February 2001; Vienna, Austria.

[21] Matz G. On non-WSSUS wireless fading channels. IEEE T Wirel Commun 2005; 4: 2465-2478.

[22] Chude-Okonkwo UA, Ngah R, Rahman TA. Time-scale domain characterization of non-WSSUS wideband channels. EURASIP J Adv Sig Pr 2011; 2011: 123.

[23] Chen Y, Zhang J, Jayalath ADS. Multiband-OFDM UWB vs IEEE802.11n: system level design considerations. In: 2006 IEEE 63rd Vehicular Technology Conference; 7–10 May 2006; Victoria, Australia. pp. 1972-1976.

[24] Capoglu IR, Li Y, Swami A. Effect of Doppler spread in OFDM-based UWB systems. IEEE T Wirel Commun 2005; 4: 2559-2567.

[25] IEEE P802.15 Working Group for Wireless Personal Area Networks. Physical Layer Submission to 802.15 Task Group 3a: Multi-Band Orthogonal Frequency Division Multiplexing. New York, NY, USA: IEEE, 2003.

[26] Batra A, Balakrishnan J, Aiello GR, Foerster JR, Dabak A. Design of a multiband OFDM system for realistic UWB channel environments. IEEE T Microw Theory 2004; 52: 2123-2138.